

## Fields of Aberrant CpG Island Hypermethylation in Barrett's Esophagus and Associated Adenocarcinoma<sup>1</sup>

Cindy A. Eads, Reginald V. Lord, Soudamini K. Kurumboor, Kumari Wickramasinghe, Margaret L. Skinner, Tiffany I. Long, Jeffrey H. Peters, Tom R. DeMeester, Kathleen D. Danenberg, Peter V. Danenberg, Peter W. Laird,<sup>2,3</sup> and Kristin A. Skinner<sup>2</sup>

Departments of Surgery [C. A. E., R. V. L., S. K. K., M. L. S., T. I. L., J. H. P., T. R. D., P. W. L., K. A. S.], Biochemistry and Molecular Biology [C. A. E., T. I. L., K. D. D., P. V. D., P. W. L.], and Pathology [K. W.], University of Southern California, Keck School of Medicine, Norris Comprehensive Cancer Center, Los Angeles, California 90089-9176

### Abstract

Esophageal adenocarcinoma (EAC) is thought to develop through a multistage process in which Barrett's metaplasia progresses through low- and high-grade dysplasia to invasive cancer. Transcriptional silencing of tumor suppressor genes by promoter CpG island hypermethylation has been observed in many types of human cancer. Analysis of CpG island hypermethylation in EAC has thus far been limited to the *CDKN2A* (p16) gene. In this study, we extend the methylation analysis of EAC to include three other genes, *APC*, *CDHI* (E-cadherin), and *ESRI* (*ER*, estrogen receptor  $\alpha$ ), in addition to *CDKN2A*. Molecular analysis can provide insight into the complex relationships between tissues with different histologies in Barrett's esophagus and associated adenocarcinoma. Therefore, we have mapped the spatial distribution of methylation patterns in six esophagectomy cases in detail. Hypermethylation of the four CpG islands was analyzed by the MethyLight technique in 107 biopsies derived from these six patients for a total of 428 methylation analyses. Our results show that normal esophageal squamous epithelium is unmethylated at all four CpG islands. *CDHI* is unmethylated in most other tissue types as well. Hypermethylation of *ESRI* is seen at high frequency in inflammatory reflux esophagitis and at all subsequent stages, whereas *APC* and *CDKN2A* hypermethylation is found in Barrett's metaplasia, dysplasia, and EAC. When it occurs, hypermethylation of *APC*, *CDKN2A*, and *ESRI* is usually found in a large contiguous field, suggesting either a concerted methylation change associated with metaplasia or a clonal expansion of cells with abnormal hypermethylation.

### Introduction

The incidence of EAC<sup>4</sup> has increased significantly in the Western world over the last three decades (1). EAC is thought to evolve from a multistep process whereby the normal esophageal squamous epithelium is replaced by specialized columnar epithelium in Barrett's esophagus (IM), followed by progression through LGD and HGD stages to invasive cancer (2). This complex sequence of events provides an excellent system to study the molecular events associated with defined histological change (3). Several reports have described genetic alterations in this system, including aneuploidy and LOH, mutation or homozygous deletion of the tumor-suppressor genes *APC*, *CDKN2A* (p16), *TP53*, and *RBI* (3–10). However, genetic alterations

could not always fully account for the inactivation of both alleles of these tumor suppressor genes. For instance, LOH at the *APC* locus has been observed in 85% of informative EAC, but mutations in the remaining allele were detected infrequently (3, 4, 6, 8, 10, 11). Reduced levels of *CDHI* (E-cadherin) protein expression have been observed in dysplastic Barrett's and EAC relative to normal esophageal epithelium (12–14). LOH of the *CDHI* locus was found in 65% of EAC cases, but mutations were rare (15). This suggests that other, nongenetic events could contribute to gene inactivation in esophageal adenocarcinoma. It is known that abnormal hypermethylation of CpG islands associated with tumor suppressor genes can lead to transcriptional silencing, providing an alternative mechanism for gene inactivation in cancer cells (16, 17). Evidence for this mechanism of gene inactivation in esophageal adenocarcinoma was provided by the documentation of promoter CpG island hypermethylation of the *CDKN2A* gene in tumors with *CDKN2A* LOH but lacking mutations in the remaining allele (18, 19). The low frequency of mutations accompanying LOH at the *APC* and *CDHI* loci may indicate that the contribution by DNA hypermethylation is more widespread in Barrett's-associated esophageal adenocarcinoma. Therefore, we have extended the analysis of DNA hypermethylation in Barrett's-associated adenocarcinoma to include 5' CpG islands associated with the *APC*, *CDHI*, and *ESRI* genes, in addition to *CDKN2A*. These CpG islands are known to become hypermethylated in adenocarcinomas of other parts of the gastrointestinal tract (20–23) and are good candidates to study DNA methylation changes in esophageal adenocarcinoma.

We have used the analysis of hypermethylation of these four CpG islands to address two separate issues: (a) in a limited number of patients, we have determined which DNA methylation changes are associated with specific histologies; (b) in each patient, we have extensively characterized how these methylation changes are distributed throughout each type of tissue. Such a study of the heterogeneity of methylation patterns within histologies, preserving the precise topological context of the tissue samples relative to each other, has not been reported previously and should add to our understanding of the molecular evolution of Barrett's-associated esophageal adenocarcinoma. To achieve this detailed analysis of methylation abnormalities, we collected between 7 and 27 biopsies from the esophagus and stomach of six esophagectomy cases, using a 1-cm grid to preserve their topological context, for a total of 107 biopsies. We determined the methylation status of the four CpG islands in each of these samples by MethyLight (23, 24). We report for the first time the hypermethylation of *APC* and *ESRI* in EAC and confirm the hypermethylation of *CDKN2A* in this system. Our results indicate that in patients with dysplasia and/or EAC, abnormal hypermethylation occurs both in the dysplastic and malignant tissues, as well as in earlier stage tissues, such as Barrett's metaplasia. Aberrant methylation is very rarely seen in the normal squamous epithelium of the esophagus.

Received 2/24/00; accepted 8/4/00.

The costs of publication of this article were defrayed in part by the payment of page charges. This article must therefore be hereby marked *advertisement* in accordance with 18 U.S.C. Section 1734 solely to indicate this fact.

<sup>1</sup> Supported by American Cancer Society Grant RPG-98-214-01-CCE (to K. A. S.) and NIH/National Cancer Institute Grant R01-CA-75090 (to P. W. L.).

<sup>2</sup> These authors contributed equally to this work.

<sup>3</sup> To whom requests for reprints should be addressed, at University of Southern California, Norris Comprehensive Cancer Center, Room 6418, 1441 Eastlake Avenue, Los Angeles, CA 90089-9176. Phone: (323) 865-0650; Fax: (323) 865-0158; E-mail: plaird@hsc.usc.edu.

<sup>4</sup> The abbreviations used are: EAC, esophageal adenocarcinoma; IM, intestinal metaplasia; LGD, low-grade dysplasia; HGD, high-grade dysplasia; LOH, loss of heterozygosity; 6FAM, 6-carboxy-fluorescein; TAMRA, 6-carboxy-tetramethylrhodamine.

The hypermethylation patterns are present throughout Barrett's esophagus and EAC tissue as a contiguous field, suggesting either a concerted alteration of DNA methylation patterns associated with metaplasia or a clonal expansion of cells with abnormal hypermethylation of CpG islands.

## Materials and Methods

**Sample Collection.** Multiple tissue samples from six patients [three males and three females; median age, 69 years (range, 47–80)] who underwent esophagectomy for adenocarcinoma ( $n = 4$ ) or for Barrett's esophagus with HGD ( $n = 2$ , patients 16 and 18) were collected fresh and immediately frozen in liquid nitrogen. The esophagectomy specimen was photographed and traced out on a 1-cm grid, marking the sites of biopsy to preserve the topographic relationships between biopsies. Biopsies from areas of visible Barrett's esophagus or cancer and from adjacent and nonadjacent areas of macroscopically normal esophageal and gastric mucosa were taken using a sterile 6-mm skin biopsy punch (Miltex, Tuttlingen, Germany). The samples were taken at 1-cm (patients 16 and 17) or 2-cm (patients 18 and 19) intervals from abnormal and adjacent normal areas or at 1-cm intervals from both adjacent and separate areas (patients 50 and 51). Part of the specimen was fixed in formalin and paraffin for histopathological examination by a single pathologist (K. W.). Frozen section examination of the study tissue was performed if the diagnosis was uncertain. The specimens were classified according to the highest grade histopathological lesion present. The diagnosis of cardiac mucosa required the presence of a columnar mucosa with glands containing mucous cells but no parietal or chief cells. All areas of cardiac mucosa showed inflammation ("carditis"), as is usual (25). The diagnosis of reflux esophagitis was made if intraepithelial eosinophils, papillary elongation, and basal hyperplasia were all present within squamous epithelium.

The site of origin of the cancers was classified as esophageal if the epicenter of the tumor was above the anatomical gastroesophageal junction, with the junction defined as the proximal margin of the gastric rugal folds. Patient 51 was classified as having a junctional (syn. cardia) cancer because the epicenter was situated at the gastroesophageal junction. TNM stages and grades of differentiation for the cancer patients were: stage 1, moderately well differentiated (patient 19); stage 2B, poorly differentiated (patient 50); stage 4A (celiac node metastasis), moderately well differentiated (patient 51); and stage 4A, poorly differentiated (patient 17). Approval for this study was obtained from the Institutional Review Board of the University of Southern California Keck School of Medicine.

**Nucleic Acid Isolation.** Genomic DNA was isolated by the standard method of proteinase K digestion and phenol-chloroform extraction (26).

**Sodium Bisulfite Conversion.** Sodium bisulfite conversion of genomic DNA was performed as described previously (27). The beads were incubated for 14 h at 50°C to ensure complete conversion.

**Methylation Analysis.** After sodium bisulfite conversion, genomic DNA was analyzed by the MethyLight technique (23, 24). Three oligos were used in every reaction: two locus-specific PCR primers flanking an oligonucleotide probe with a 5' fluorescent reporter dye (6FAM) and a 3' quencher dye (TAMRA; Ref. 28). The PCR amplification was performed as described previously (23, 24). Two sets of primers and probes, designed specifically for bisulfite-converted DNA, were used: a methylated set for the gene of interest [*APC*, *CDHI*, *CDKN2A* (p16), or *ESRI*], each spanning from 7 to 10 CpG dinucleotides, and a reference set,  $\beta$ -actin (*ACTB*), to normalize for input DNA. Specificity of the reactions for methylated DNA were confirmed separately using human sperm DNA (unmethylated) and *SssI* (New England Biolabs) treated sperm DNA (methylated). The reference primers and the probe were designed in a region of the *ACTB* gene that lacks any CpG dinucleotides to allow for equal amplification, regardless of methylation levels. Parallel TaqMan PCR reactions were performed with primers specific for the bisulfite-converted methylated sequence for a particular locus and with the *ACTB* reference primers. The ratio between the values obtained in these two TaqMan analyses was used as a measure for the degree of methylation at that locus. The percentage of fully methylated molecules at a specific locus was calculated by dividing the *GENE:ACTB* ratio of a sample by the *GENE:ACTB* ratio of *SssI*-treated sperm DNA and multiplying by 100. Samples containing  $\geq 4\%$  fully methylated molecules were designated as methylated, whereas samples containing  $< 4\%$  were designated as unmethylated. The 4% cutoff

gave the best discrimination between normal and premalignant/malignant tissues. The primer and probe sequences are listed below. In all cases, the first primer listed is the forward PCR primer, the second is the TaqMan probe, and the third is the reverse PCR primer. The GenBank accession number and amplicon location for each reaction are indicated between parentheses; *APC* (U02509, 759–832), GAACCAAAACGCTCCCCAT, 6FAM5'-CCCGTCGAA-AACCCGCCGATTA-3'TAMRA, TTATATGTCGGTTACGTGCGTTTATAT; *CDHI* (L34545, 842–911), AATTTTAGGTTAGAGGGTTATCGCGT, 6FAM5'-CGCCACCCGACCTCGCAT-3'TAMRA, TCCCCAAAACGAAACTAACGAC; *CDKN2A* (NM\_000077, 66–133, there are two bases in our primers that differ from this GenBank sequence, because a preliminary high-throughput GenBank entry was the only available sequence at the time of our primer design), TGGAATTTTCGGTTGATTGGTT, 6FAM5'-ACCCGACCCCGAACCGCG-3'TAMRA, AACAACGTCCGCACCTCT; *ESRI* (X62462, 2784–2884) GCGGTTTCGTTTGGGATTG, 6FAM5'-CGATAAAAACCGAACGACCCGACGA-3'TAMRA, GCCGACACGCGAACTCTAA; and *ACTB* (Y00474, 390–522), TGGTGATGGAGGAGGTTTAGTAAGT, 6FAM5'-ACCACCACC-CAACACACAATAACAAACACA-3'TAMRA, AACCAATAAAACCTACTCTCCCTTAA.

## Results

We selected CpG islands located in the 5' regions of the *APC*, *CDHI*, *CDKN2A*, and *ESRI* genes to examine the methylation patterns in the progression of EAC. A quantitative, fluorescence-based (TaqMan) bisulfite-PCR method called MethyLight was used (23, 24). Briefly, methylation-specific oligos were designed to amplify completely methylated molecules. The reaction for each specific gene (*APC*, *CDHI*, *CDKN2A*, or *ESRI*) was run in parallel with a reference reaction ( $\beta$ -actin, *ACTB*) to correct for input DNA for each sample. The ratio between the gene of interest and the reference gene is indicative of the relative prevalence of fully methylated molecules in a given sample. The efficiencies of our methylation reactions are controlled for in each analysis by including unmethylated control DNA and fully methylated control DNA (Fig. 1, A and B). As shown for the unmethylated control, only the reference gene (*ACTB*) amplifies, whereas all reactions showed amplification in the fully methylated control DNA, as expected. This discrimination allows us to detect fully methylated molecules in heterogeneous samples such as normal and tumor esophageal tissue (Fig. 1, C and D). Fig. 1C demonstrates that for a representative normal esophageal mucosa tissue, the reference reaction (*ACTB*) amplifies, whereas *APC*, *CDHI*, *CDKN2A*, and *ESRI* specific oligos do not, indicating a lack of methylation at these CpG islands in this normal sample. In the matched EAC sample, however, *APC* and *ESRI* amplify along with *ACTB*, whereas *CDKN2A* and *CDHI* are negative, indicating *APC*- and *ESRI*-specific hypermethylation (Fig. 1D).

The methylation results of *APC*, *CDHI*, *CDKN2A*, and *ESRI* obtained from the four most extensive mappings of the six esophagectomy patients (cases 16, 17, 50, and 51) are depicted in Fig. 2. The results for the other two mappings (cases 18 and 19) are summarized in Table 1. Each case contains a unique combination and topography of various tissue types. All four genes are unmethylated in almost all normal esophageal mucosa samples (Fig. 2 and Table 1). *CDHI* is rarely methylated in any tissue. It is most commonly methylated in normal stomach (24%; Table 1), which is consistent with a previous report of occasional *CDHI* methylation in gastric mucosa (22). *APC* and *ESRI* are methylated in the majority of Barrett's metaplastic and dysplastic samples and/or adenocarcinoma samples (Fig. 2). *APC* hypermethylation is present throughout the Barrett's IM (cases 16 and 17), whereas *ESRI* hypermethylation is found ubiquitously in adenocarcinoma tissue (cases 17, 50, and 51). *APC* is also frequently methylated (76%) in the normal stomach in every patient (Table 1). *APC* and *ESRI* methylation changes are even detected in samples of reflux esophagitis and cardiac mucosa in case 16 (Fig. 2; Table 1).



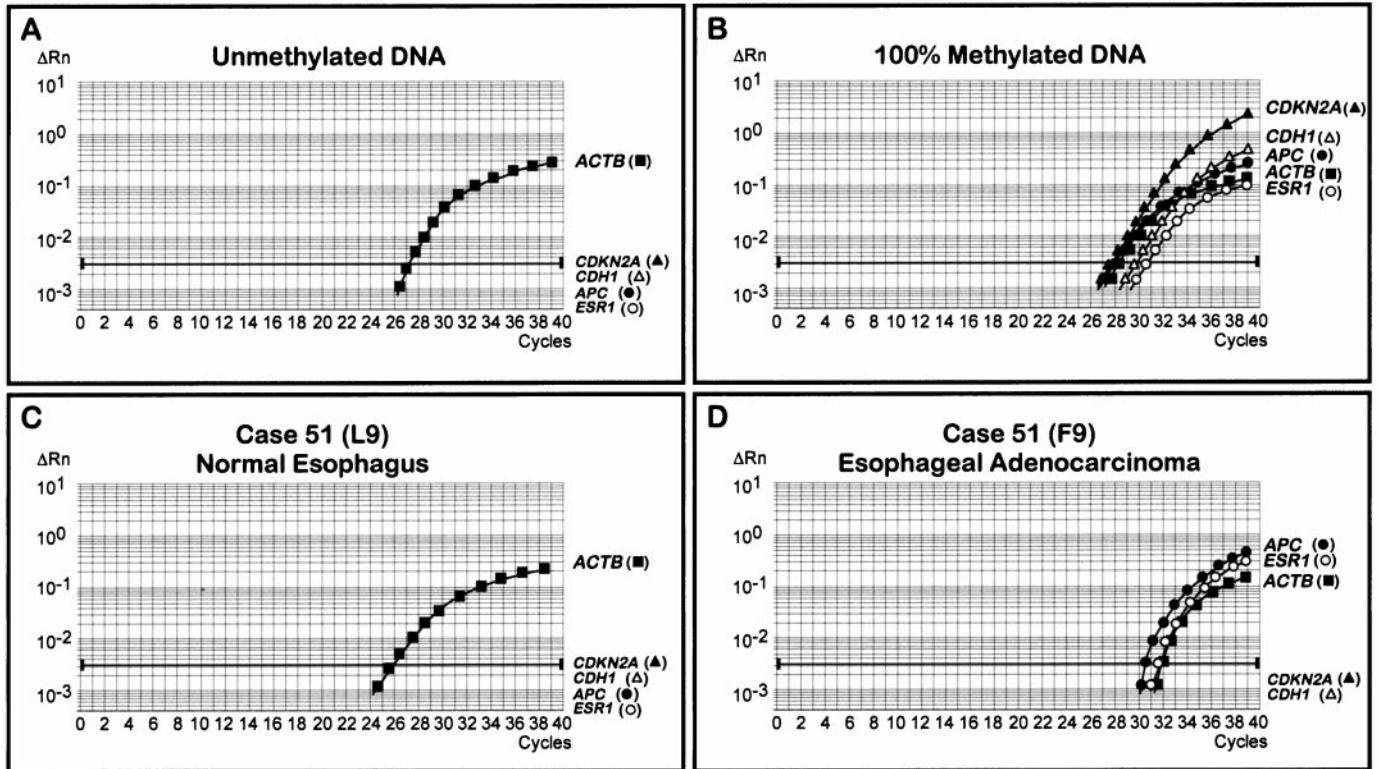


Fig. 1. Methylation analysis of *APC*, *CDH1*, *CDKN2A*, and *ESR1* using fluorescence-based, quantitative, real-time PCR (TaqMan). In the PCR reaction, an oligonucleotide probe tagged with a 5' fluorescent reporter and 3' quencher is added in addition to the standard PCR components. As the Taq polymerase synthesizes the new strand, its 5' to 3' nuclease activity cleaves the probe, separating the quencher and fluorescent reporter. The fluorescence emitted is proportional to the amount of product accumulated with each cycle. *Horizontal bold line*, fluorescence level used for the threshold cycle determination in this particular example.  $\Delta Rn$  is defined as the cycle-to-cycle change in the reporter fluorescence signal normalized to a passive reference fluorescence signal. Two sets of primers and probes, designed specifically for bisulfite-converted DNA, were used: a methylated set for the gene of interest [*APC*, *CDH1*, *CDKN2A* (p16), or *ESR1*] and a reference set (*ACTB*) to control for input DNA. Specificity of the reactions for methylated DNA were confirmed separately using sperm DNA (unmethylated; A) and *SssI*-treated sperm DNA (methylated; B). C and D show a representative analysis from a normal esophageal mucosa sample and a matched esophageal adenocarcinoma sample from case 51. L9 and F9 designate the sample location in Fig. 2.

*CDKN2A* hypermethylation is observed only in cases 16 and 17. Both tumor samples in case 17 show *CDKN2A* hypermethylation. It is detected throughout the metaplastic and dysplastic Barrett's tissues in case 16 and in some samples of IM, LGD, and adenocarcinoma in case 17 (Fig. 2; Table 1).

Both *APC* and *CDKN2A* methylation are found at higher frequency in Barrett's tissues than in the adenocarcinoma samples (Table 1). This could be attributable to the reversible nature of DNA methylation, as other events such as mutation take over in the tumor. Alternatively, the decreased methylation signal could reflect the deletion of methylated alleles attributable to LOH of *APC* and/or *CDKN2A* in the adenocarcinoma samples. Either of these scenarios would be consistent with DNA methylation acting as an early-stage inactivation mechanism that is later supplanted by irreversible genetic events (29). In contrast, *ESR1* methylation is retained in all adenocarcinoma samples. The *ESR1* gene is not a classical tumor suppressor gene and does not commonly undergo LOH or mutational events.

## Discussion

Previous studies of hypermethylation in Barrett's esophagus and EAC have been limited to the *CDKN2A* gene and have focused on the analysis of a very small number of samples from each patient with Barrett's esophagus and/or esophageal adenocarcinoma. In this study, we have used an alternative approach that not only documents the occurrence of hypermethylation of four CpG islands (*APC*, *CDH1*, *CDKN2A*, and *ESR1*) but also provides the topological context in which this hypermethylation occurs in histologically defined areas of

Barrett's-associated EAC. Because this experimental approach by necessity involves the analysis of a large number of samples per patient, we have restricted the number of cases to six. Although the limited number of patients does not allow us to extrapolate on the general occurrence of hypermethylation of these four genes in Barrett's-associated EAC, this alternative strategy revealed interesting trends.

Our results demonstrate two important points:

(a) Abnormal methylation patterns are not restricted to the adenocarcinoma tissue but are also found in premalignant Barrett's tissue. This suggests that DNA hypermethylation is an early epigenetic alteration in the multistep progression of EAC. We have argued previously that the features of DNA methylation are particularly well suited for a role early in the cancer process (29). An early role for DNA methylation in gastrointestinal tumors is further supported by the observation that polyp formation in *Apc*<sup>Min/+</sup> mice is dependent upon sufficient levels of DNA methyltransferase activity early in polyp development (30).

(b) These aberrant methylation patterns tend to occur in large contiguous fields. This would be expected for a monoclonally expanded tissue such as an adenocarcinoma. It has been reported that the clonal status of Barrett's IM is related to the proximity of dysplastic or malignant tissue (3). However, some of the nondysplastic IM samples with widespread hypermethylation in our study do not show evidence of dysplasia in adjacent biopsies located 1 cm away (e.g., both samples B1 in cases 16 and 17). Therefore, some of the concerted hypermethylation observed in IM in our study may represent a non-

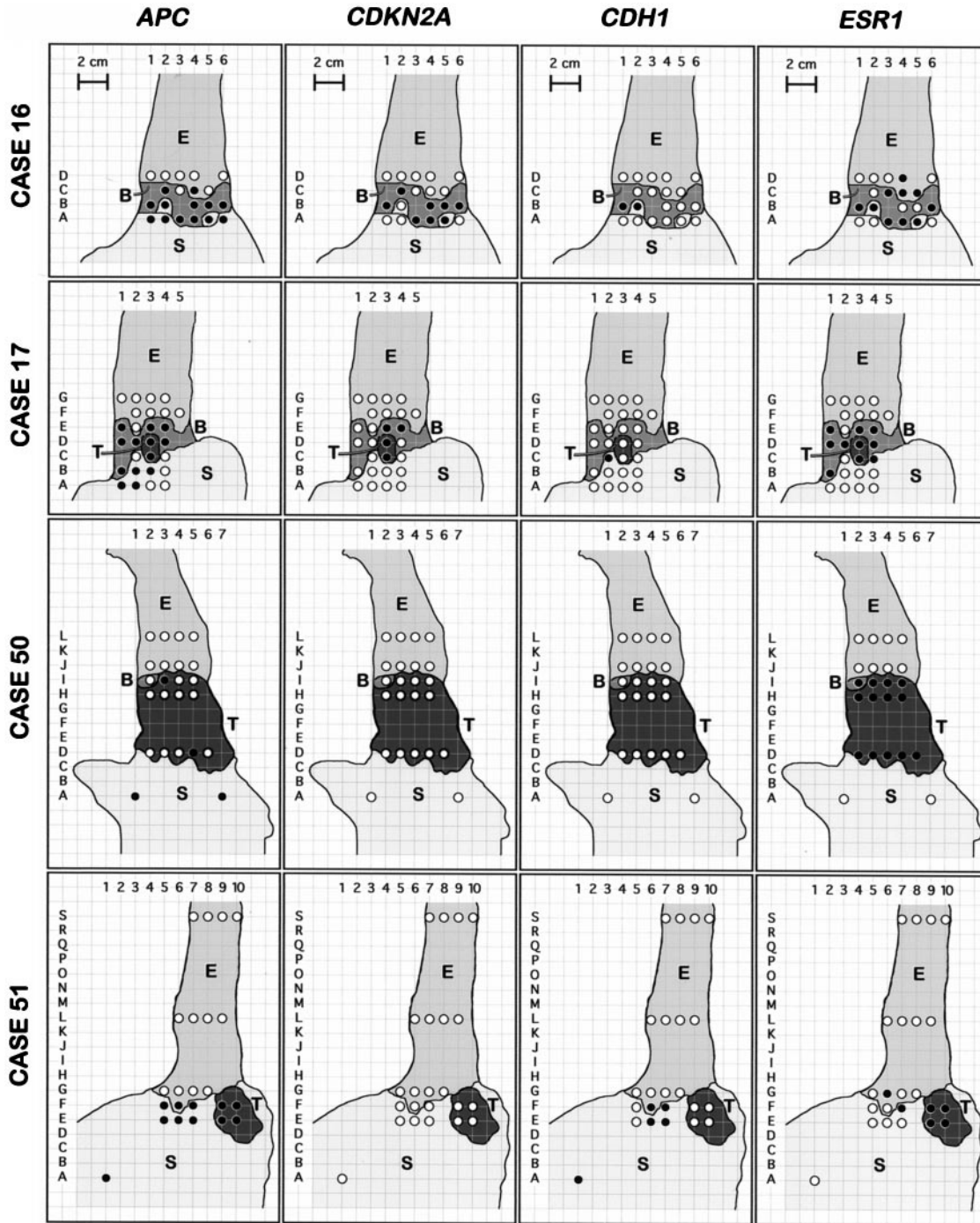


Fig. 2. Schematic of methylation results obtained from four esophagectomy patients. The esophagus for each case (cases 16, 17, 50, and 51) is illustrated to scale in each row, with the distance between points on the grid being 1 cm. The different tissue types are designated as varying degrees of gray and labeled with a corresponding letter (*E*, normal esophageal mucosa; *S*, stomach; *B*, Barrett's esophagus; *T*, adenocarcinoma). The methylation status of *APC*, *CDH1*, *CDKN2A* (p16), or *ESR1* is shown in each column. Each circle represents a 6-mm punch biopsy. ●, samples in which >4% of the DNA molecules analyzed have full methylation of all of the CpG dinucleotides covered by the respective assay. ○, those samples in which this value was  $\geq 4\%$ . Case 16 has normal squamous epithelium (*D1*–3, 6), normal stomach (*A1*–2, 6), reflux esophagitis (*C4*, 5 and *D4*), cardiac mucosa (*A5* and *B2*), Barrett's IM (*A4*; *B1*, 4, 5; and *C2*), Barrett's with LGD (*B6* and *C3*) and HGD (*A3*) but lacks adenocarcinoma tissue. Case 17 has normal squamous epithelium (*E2*; *F2*–5; and *G1*–4), and normal stomach (*A1*–4; *B2*–4; and *C2*, 4), Barrett's IM (*B1*; *D2*, 4; and *E3*), LGD (*D1* and *E1*, 4), and adenocarcinoma (*C3* and *D3*). Case 50 has normal esophageal squamous epithelium (*J2*–5 and *L2*–5) and normal stomach (*A1*, 7), one sample of Barrett's IM (*I2*), and adenocarcinoma (*D2*–6; *H2*–5; and *I3*–5). Case 51 has normal esophageal squamous epithelium (*F6*; *G5*–8; *L6*–9; and *S7*–10), normal stomach (*A1*; *E5*–7; and *F5*, 7), and adenocarcinoma (*E9*–10; and *F9*–10).

monoclonal process, associated with metaplasia or ongoing repetitive injury, rather than clonal expansion. For instance, the *APC* hypermethylation observed in Barrett's tissue may be a consequence of the metaplastic change to columnar epithelium, because it is also frequently found to be methylated in the normal columnar epithelium of the stomach, whereas the hypermethylation observed in the esopha-

gitis samples could indicate changes associated with chronic reflux-induced damage to the squamous mucosa. Such nonclonal changes might create a field of abnormal hypermethylation that predisposes the tissue to further progression. On the other hand, it is also possible that the contiguous methylation patterns observed in the Barrett's tissue represent a clonal expansion of a hypermethylated cell. Many

Table 1 Frequency of CpG island hypermethylation for different tissue types

| Gene and tissue | Case 16 | Case 17 | Case 18         | Case 19 | Case 50 | Case 51 | Total | Total % |
|-----------------|---------|---------|-----------------|---------|---------|---------|-------|---------|
| <b>APC</b>      |         |         |                 |         |         |         |       |         |
| Stomach         | 3/3     | 4/9     | NA <sup>a</sup> | 1/1     | 2/2     | 6/6     | 16/21 | 76      |
| Esophagus       | 0/4     | 0/9     | 0/3             | 0/2     | 0/8     | 1/13    | 1/39  | 3       |
| Esophagitis     | 1/3     | NA      | 0/1             | NA      | NA      | NA      | 1/4   | 25      |
| Cardiac mucosa  | 2/2     | NA      | NA              | NA      | NA      | NA      | 2/2   | 100     |
| Barrett's IM    | 5/5     | 4/4     | 0/1             | 2/2     | 0/1     | NA      | 11/13 | 85      |
| Barrett's LGD   | 1/2     | 3/3     | NA              | 1/1     | NA      | NA      | 5/6   | 83      |
| Barrett's HGD   | 1/1     | NA      | 1/2             | NA      | NA      | NA      | 2/3   | 66      |
| Tumor           | NA      | 2/2     | NA              | 0/1     | 2/12    | 4/4     | 8/19  | 42      |
| <b>CDKN2A</b>   |         |         |                 |         |         |         |       |         |
| Stomach         | 0/3     | 0/9     | NA              | 0/1     | 0/2     | 0/6     | 0/21  | 0       |
| Esophagus       | 0/4     | 0/9     | 0/3             | 0/2     | 0/8     | 0/13    | 0/39  | 0       |
| Esophagitis     | 0/3     | NA      | 0/1             | NA      | NA      | NA      | 0/4   | 0       |
| Cardiac mucosa  | 1/2     | NA      | NA              | NA      | NA      | NA      | 1/2   | 50      |
| Barrett's IM    | 5/5     | 1/4     | 0/1             | 0/2     | 0/1     | NA      | 6/13  | 46      |
| Barrett's LGD   | 1/2     | 1/3     | NA              | 0/1     | NA      | NA      | 2/6   | 33      |
| Barrett's HGD   | 1/1     | NA      | 0/2             | NA      | NA      | NA      | 1/3   | 33      |
| Tumor           | NA      | 2/2     | NA              | 1/1     | 0/12    | 0/4     | 3/19  | 16      |
| <b>CDH1</b>     |         |         |                 |         |         |         |       |         |
| Stomach         | 0/3     | 1/9     | NA              | 0/1     | 0/2     | 4/6     | 5/21  | 24      |
| Esophagus       | 0/4     | 0/9     | 0/3             | 0/2     | 0/8     | 1/13    | 1/39  | 3       |
| Esophagitis     | 0/3     | NA      | 0/1             | NA      | NA      | NA      | 0/4   | 0       |
| Cardiac mucosa  | 1/2     | NA      | NA              | NA      | NA      | NA      | 1/2   | 50      |
| Barrett's IM    | 1/5     | 0/4     | 0/1             | 0/2     | 0/1     | NA      | 1/13  | 8       |
| Barrett's LGD   | 0/2     | 0/3     | NA              | 0/1     | NA      | NA      | 0/6   | 0       |
| Barrett's HGD   | 0/1     | NA      | 0/2             | NA      | NA      | NA      | 0/3   | 0       |
| Tumor           | NA      | 0/2     | NA              | 0/1     | 0/12    | 0/4     | 0/19  | 0       |
| <b>ESR1</b>     |         |         |                 |         |         |         |       |         |
| Stomach         | 0/3     | 1/9     | NA              | 0/1     | 0/2     | 1/6     | 2/21  | 10      |
| Esophagus       | 0/4     | 0/9     | 0/3             | 1/2     | 0/8     | 1/13    | 2/39  | 5       |
| Esophagitis     | 3/3     | NA      | 0/1             | NA      | NA      | NA      | 3/4   | 75      |
| Cardiac mucosa  | 2/2     | NA      | NA              | NA      | NA      | NA      | 2/2   | 100     |
| Barrett's IM    | 2/5     | 4/4     | 0/1             | 2/2     | 1/1     | NA      | 9/13  | 69      |
| Barrett's LGD   | 2/2     | 3/3     | NA              | 1/1     | NA      | NA      | 6/6   | 100     |
| Barrett's HGD   | 1/1     | NA      | 1/2             | NA      | NA      | NA      | 2/3   | 67      |
| Tumor           | NA      | 2/2     | NA              | 1/1     | 12/12   | 4/4     | 19/19 | 100     |

<sup>a</sup> NA, not applicable.

studies have reported LOH or mutations of *APC*, *TP53*, and *CDKN2A* that support a clonal expansion in premalignant Barrett's esophagus (3, 8, 9). These molecular events have usually been found to be associated with dysplasia. Our results show the frequent and widespread occurrence of aberrant methylation patterns in nondysplastic tissues. However, all of the cases that we have investigated also have associated HGD and/or adenocarcinoma. It is possible that nondysplastic tissues in individuals with IM as their most advanced stage of disease would not show such aberrant hypermethylation. Such patients are not included in our study, because they do not undergo esophagectomy.

The clonality of a tissue can be determined by tracing a specific mutation or LOH event through the different stages of EAC or, in female patients, by analyzing the homogeneity of X-chromosomal inactivation in the tissue sample (3). Barrett's tissue is very heterogeneous and requires cell sorting to remove contaminating normal cells for an accurate detection of clonality. Because our tissue specimens were not microdissected or cell sorted, we are unable to determine the clonality in the fields of DNA hypermethylation. The presence of substantial amounts of normal tissue in our specimens also prevents an assessment of the gene inactivation effects of the CpG island hypermethylation that we have detected. Gene expression in the normal stromal and epithelial cells in the specimen can mask a lack of expression in a subset of cells with CpG island hypermethylation. Indeed, samples from our study with substantial levels of complete methylation of the *CDKN2A* promoter CpG island still showed significant *CDKN2A* gene expression, as analyzed by quantitative real-time reverse transcription-PCR (data not shown), despite the fact that there is strong evidence for the gene silencing effects of *CDKN2A* promoter CpG island hypermethylation in more homogeneous tissues and cell lines (31). Similar results showing a lack of

clear inverse correlation between the methylation and gene expression data were obtained for *APC* and *ESR1* as well (data not shown). Therefore, we believe that the analysis of aberrant DNA hypermethylation offers an advantage over deletion analysis and gene expression analysis in that it has greater sensitivity in the presence of contaminating normal cells. This alleviates the need for cell sorted populations and microdissected tissue samples, which are generally used in LOH and deletion studies of esophageal tumors.

Regardless of whether the observed CpG island hypermethylation events are attributable to field effects that arise from either clonal expansion or nonclonal concerted changes, it is clear that aberrant methylation patterns can occur in early-stage tissues associated with dysplasia and/or malignancy. A prospective longitudinal study should reveal whether these molecular alterations in early-stage tissues are predictive of imminent dysplastic disease.

## Acknowledgments

We thank David VandenBerg for advice on the design of Fig. 2.

## References

- Devesa, S. S., Blot, W. J., and Fraumeni, J. F., Jr. Changing patterns in the incidence of esophageal and gastric carcinoma in the United States. *Cancer (Phila.)*, 83: 2049–2053, 1998.
- Jankowski, J. A., Wright, N. A., Meltzer, S. J., Triadafilopoulos, G., Geboes, K., Casson, A. G., Kerr, D., and Young, L. S. Molecular evolution of the metaplasia-dysplasia-adenocarcinoma sequence in the esophagus. *Am. J. Pathol.*, 154: 965–973, 1999.
- Zhuang, Z., Vortmeyer, A. O., Mark, E. J., Odze, R., Emmert-Buck, M. R., Merino, M. J., Moon, H., Liotta, L. A., and Duray, P. H. Barrett's esophagus: metaplastic cells with loss of heterozygosity at the *APC* gene locus are clonal precursors to invasive adenocarcinoma. *Cancer Res.*, 56: 1961–1964, 1996.
- Boynton, R. F., Blount, P. L., Yin, J., Brown, V. L., Huang, Y., Tong, Y., McDaniel, T., Newkirk, C., Resau, J. H., and Raskind, W. H. Loss of heterozygosity involving the *APC* and *MCC* genetic loci occurs in the majority of human esophageal cancers. *Proc. Natl. Acad. Sci. USA*, 89: 3385–3388, 1992.



5. Huang, Y., Meltzer, S. J., Yin, J., Tong, Y., Chang, E. H., Srivastava, S., McDaniel, T., Boynton, R. F., and Zou, Z. Q. Altered messenger RNA and unique mutational profiles of p53 and Rb in human esophageal carcinomas. *Cancer Res.*, *53*: 1889–1894, 1993.
6. Huang, Y., Boynton, R. F., Blount, P. L., Silverstein, R. J., Yin, J., Tong, Y., McDaniel, T. K., Newkirk, C., Resau, J. H., Sridhara, R., *et al.* Loss of heterozygosity involves multiple tumor suppressor genes in human esophageal cancers. *Cancer Res.*, *52*: 6525–6530, 1992.
7. Barrett, M. T., Sanchez, C. A., Galipeau, P. C., Neshat, K., Emond, M., and Reid, B. J. Allelic loss of 9p21 and mutation of the *CDKN2/p16* gene develop as early lesions during neoplastic progression in Barrett's esophagus. *Oncogene*, *13*: 1867–1873, 1996.
8. Barrett, M. T., Sanchez, C. A., Prevo, L. J., Wong, D. J., Galipeau, P. C., Paulson, T. G., Rabinovitch, P. S., and Reid, B. J. Evolution of neoplastic cell lineages in Barrett oesophagus. *Nat. Genet.*, *22*: 106–109, 1999.
9. Prevo, L. J., Sanchez, C. A., Galipeau, P. C., and Reid, B. J. p53-mutant clones and field effects in Barrett's esophagus. *Cancer Res.*, *59*: 4784–4787, 1999.
10. Gonzalez, M. V., Artinez, M. L., Rodrigo, L., Lopez-Larrea, C., Menendez, M. J., Alvarez, V., Perez, R., Fresno, M. F., Perez, M. J., Sampetro, A., and Coto, E. Mutation analysis of the p53, APC, and p16 genes in the Barrett's oesophagus, dysplasia, and adenocarcinoma. *J. Clin. Pathol.*, *50*: 212–217, 1997.
11. Powell, S. M., Papadopoulos, N., Kinzler, K. W., Smolinski, K. N., and Meltzer, S. J. APC gene mutations in the mutation cluster region are rare in esophageal cancers. *Gastroenterology*, *107*: 1759–1763, 1994.
12. Bongiorno, P. F., al-Kasspoles, M., Lee, S. W., Rachwal, W. J., Moore, J. H., Whyte, R. I., Orringer, M. B., and Beer, D. G. E-Cadherin expression in primary and metastatic thoracic neoplasms and in Barrett's oesophagus. *Br. J. Cancer*, *71*: 166–172, 1995.
13. Swami, S., Kumble, S., and Triadafilopoulos, G. E-Cadherin expression in gastroesophageal reflux disease, Barrett's esophagus, and esophageal adenocarcinoma: an immunohistochemical and immunoblot study. *Am. J. Gastroenterol.*, *90*: 1808–1813, 1995.
14. Washington, K., Chiappori, A., Hamilton, K., Shyr, Y., Blanke, C., Johnson, D., Sawyers, J., and Beauchamp, D. Expression of  $\beta$ -catenin,  $\alpha$ -catenin, and E-cadherin in Barrett's esophagus and esophageal adenocarcinomas. *Mod. Pathol.*, *11*: 805–813, 1998.
15. Wijnhoven, B. P., de Both, N. J., van Dekken, H., Tilanus, H. W., and Dinjens, W. N. *E-Cadherin* gene mutations are rare in adenocarcinomas of the oesophagus. *Br. J. Cancer*, *80*: 1652–1657, 1999.
16. Jones, P. A., and Laird, P. W. Cancer epigenetics comes of age. *Nat. Genet.*, *21*: 163–167, 1999.
17. Baylin, S. B., Herman, J. G., Graff, J. R., Vertino, P. M., and Issa, J. P. Alterations in DNA methylation: a fundamental aspect of neoplasia. *Adv. Cancer Res.*, *72*: 141–196, 1998.
18. Wong, D. J., Barrett, M. T., Stoger, R., Emond, M. J., and Reid, B. J. p16INK4a promoter is hypermethylated at a high frequency in esophageal adenocarcinomas. *Cancer Res.*, *57*: 2619–2622, 1997.
19. Klump, B., Hsieh, C. J., Holzmann, K., Gregor, M., and Porschen, R. Hypermethylation of the *CDKN2/p16* promoter during neoplastic progression in Barrett's esophagus. *Gastroenterology*, *115*: 1381–1386, 1998.
20. Hiltunen, M. O., Alhonen, L., Koistinaho, J., Myohanen, S., Paakkonen, M., Marin, S., Kosma, V. M., and Janne, J. Hypermethylation of the APC (adenomatous polyposis coli) gene promoter region in human colorectal carcinoma. *Int. J. Cancer*, *70*: 644–648, 1997.
21. Issa, J. P., Ottaviano, Y. L., Celano, P., Hamilton, S. R., Davidson, N. E., and Baylin, S. B. Methylation of the oestrogen receptor CpG island links aging and neoplasia in human colon. *Nat. Genet.*, *7*: 536–540, 1994.
22. Suzuki, H., Itoh, F., Toyota, M., Kikuchi, T., Kakiuchi, H., Hinoda, Y., and Imai, K. Distinct methylation pattern and microsatellite instability in sporadic gastric cancer. *Int. J. Cancer*, *83*: 309–313, 1999.
23. Eads, C. A., Danenberg, K. D., Kawakami, K., Saltz, L. B., Danenberg, P. V., and Laird, P. W. CpG island hypermethylation in human colorectal tumors is not associated with DNA methyltransferase overexpression. *Cancer Res.*, *59*: 2302–2306, 1999.
24. Eads, C. A., Danenberg, K. D., Kawakami, K., Saltz, L. B., Blake, C., Shibata, D., Danenberg, P. V., and Laird, P. W. MethyLight: a high-throughput assay to measure DNA methylation. *Nucleic Acids Res.*, *28*: E32, 2000.
25. Oberg, S., Peters, J. H., DeMeester, T. R., Chandrasoma, P., Hagen, J. A., Ireland, A. P., Ritter, M. P., Mason, R. J., Crookes, P., and Bremner, C. G. Inflammation and specialized intestinal metaplasia of cardiac mucosa is a manifestation of gastroesophageal reflux disease. *Ann. Surg.*, *226*: 522–530; discussion 530–532, 1997.
26. Wolff, R. K., Frazer, K. A., Jackler, R. K., Lanser, M. J., Pitts, L. H., and Cox, D. R. Analysis of chromosome 22 deletions in neurofibromatosis type 2-related tumors. *Am. J. Hum. Genet.*, *51*: 478–485, 1992.
27. Olek, A., Oswald, J., and Walter, J. A modified and improved method for bisulphite based cytosine methylation analysis. *Nucleic Acids Res.*, *24*: 5064–5066, 1996.
28. Livak, K. J., Flood, S. J., Marmaro, J., Giusti, W., and Deetz, K. Oligonucleotides with fluorescent dyes at opposite ends provide a quenched probe system useful for detecting PCR product and nucleic acid hybridization. *PCR Methods Applications*, *4*: 357–362, 1995.
29. Laird, P. W. Oncogenic mechanisms mediated by DNA methylation. *Mol. Med. Today*, *3*: 223–229, 1997.
30. Laird, P. W., Jackson-Grusby, L., Fazeli, A., Dickinson, S. L., Jung, W. E., Li, E., Weinberg, R. A., and Jaenisch, R. Suppression of intestinal neoplasia by DNA hypomethylation. *Cell*, *81*: 197–205, 1995.
31. Gonzalzo, M. L., Hayashida, T., Bender, C. M., Pao, M. M., Tsai, Y. C., Gonzales, F. A., Nguyen, H. D., Nguyen, T. T., and Jones, P. A. The role of DNA methylation in expression of the *p19/p16* locus in human bladder cancer cell lines. *Cancer Res.*, *58*: 1245–1252, 1998.